



# Natural vibrations of anisotropic plates with an internal curve with hinges



Javier Leandro Raffo<sup>a</sup>, Maria Virginia Quintana<sup>b</sup>

<sup>a</sup> Grupo de Mecánica Computacional, Facultad Regional Delta, Universidad Tecnológica Nacional, San Martín 1171, 2804 Campana, Argentina

<sup>b</sup> INIQUL- Facultad de Ingeniería, CONICET- Universidad Nacional de Salta, Avenida Bolivia 5150, Salta, Argentina

## ARTICLE INFO

### Keywords:

Vibration  
Anisotropic plate  
Ritz method  
Penalty function  
Internal curve  
Hinge

## ABSTRACT

The objective of this paper is to propose a general algorithm to obtain approximate analytical solutions for the study of the free vibrations of a rectangular anisotropic thin plate with an internal curved line hinge and general restraints. In this system, there exists an intermediate condition that requires the continuity of the transverse displacements. It is well known that the difficulty in choosing admissible functions has been the most significant drawback of the Ritz method. To relax the admissibility requirement the Ritz method, with polynomials as coordinate functions, in conjunction with the Penalty Function method is proposed. This study is focus on different problems related the curved hinge and a natural parametrization is used to treat the mentioned curves. The accuracy of the formulation is ensured by comparing some numerical examples with those available in the literature. Cases not previously treated are particularly analyzed. Frequencies parameters and several sets of vibration mode shapes are included, to provide a better understanding of the dynamical behavior of these plates.

## 1. Introduction

The plate is probably one of the most common structural elements that have been devised by either scientific or technological interest. It is widely encountered in aerospace, marine, mechanical and civil engineering structures. The dynamical behavior of plates is one of the major concerns in designing this type of structures. It is not the intention to review the literature, consequently only some of the published papers related to the present work will be cited.

Plates with different shapes, boundary conditions and complicating effects have been considered and the frequency parameters were documented in monographs [1,2], standard texts [3–5] and review papers [6,7]. Several complicating effects have been considered such as: elastically restrained boundaries, presence of elastically or rigidly connected masses, variable thickness, anisotropic material, presence of holes, etc. In references [8–11] general studies on vibration of plates with point supports have been presented and vibration of plates with line supports have been developed in references [12–14].

A review of the literature has shown that there is only a limited amount of information for the vibration of plates with line hinges. A line hinge with elastic restrictions in a plate can be used to simulate a through crack along the interior of the plate. Yuan and Dickinson [15] used the Rayleigh-Ritz approach for the study of the free vibration of systems comprised of rectangular plates. The choice of the deflection functions for the component plates were simplified through the use of

the concept of artificial springs being introduced at the joints between the plates and at the system boundaries. The necessary continuity and boundary conditions were enforced through allowing the appropriate spring stiffness to become very high compared with the stiffness of the components. Li et al. [16] investigated the vibrational power flow of circular plates with peripheral surface crack modeled as a joint of a local spring. The peripheral surface crack is modeled as a joint of a local spring. The local stiffness of the rotational spring is deduced by using fracture mechanics and strain energy arguments.

Wang et al. [17] studied the buckling and vibration of plates with an internal line hinge by using the Ritz method. Gupta and Reddy [18] studied the exact buckling loads and vibration frequencies of orthotropic rectangular plates with an internal line hinge by employing an analytical method which applies the Levy solution and the domain decomposition technique. Xiang and Reddy [19] developed the first known solution based on the first order shear deformation theory for vibration of rectangular plates with an internal line hinge. The Lévy method and the state-space technique were employed to solve the vibration problem and obtain frequency coefficients values. Huang et al. [20] presented a discrete method to analyze the free vibration problem of thin and moderately thick rectangular plates with an intermediate line hinge. Quintana and Grossi [21] dealt with the study of free transverse vibrations of isotropic rectangular plates with an internal line hinge and elastically restrained boundaries. The problem was solved employing a combination of the Ritz method and the

E-mail addresses: [jraffo@frd.utn.edu.ar](mailto:jraffo@frd.utn.edu.ar) (J.L. Raffo), [vquintan@unsa.edu.ar](mailto:vquintan@unsa.edu.ar) (M.V. Quintana).

<http://dx.doi.org/10.1016/j.ijmecsci.2016.11.031>

Received 26 May 2016; Received in revised form 24 November 2016; Accepted 30 November 2016

Available online 01 December 2016

0020-7403/ © 2016 Elsevier Ltd. All rights reserved.

Lagrange multiplier method. Grossi [22] used the Hamilton's principle for the derivation of equations of motion and its associated boundary and transition conditions of anisotropic plates with an arbitrarily located internal line hinges with elastics supports and piecewise-smooth boundaries elastically restrained against rotation and translation among other complicating effects. Grossi and Raffo [23] extended the model to analyze anisotropic plates with several arbitrarily located internal lines hinges. Finally, Quintana and Grossi [24] presented a general variational formulation for the free vibrations of laminated thin plates of trapezoidal shape with an internal line hinge. The analysis was carried out by using the kinematics corresponding to the classical laminated plate theory and the eigenvalue problem was obtained by employing a combination of the Ritz method and the Lagrange multipliers method. All of these studies have considered isotropic and anisotropic plates with internal straight lines hinges. However, the literature does not appear to contain any substantial references to analytical models for anisotropic plates with an internal curve with hinges.

According to the statement in the preceding paragraphs the objective of this paper is to propose a general algorithm to obtain approximate analytical solutions for the study of the free vibrations of a rectangular anisotropic thin plate with an internal curve with hinges and general boundary conditions. In this system, there exists an intermediate condition that requires the continuity of the displacements along the line hinge. It is well known that the difficulty in choosing admissible functions has been the most significant drawback of the Ritz method. One way to relax the admissibility requirement may be found by utilizing a constrained optimization technique known as the Lagrangian multiplier method. This method might imply a considerable computational effort. An alternative approach is the Penalty Function Method. The effectiveness of this approach has since been studied by several researchers for various interesting problems and its applicability has also been extended to analyze rigidly connected systems and systems with cracks [25,26]. Ilanko and Montterubio [27] presented the Rayleigh-Ritz method in an engineering context. The treatment is in a somewhat heuristic form. Nevertheless several textbooks include the corresponding rigorous treatment [28–30].

In this paper a methodology based on a combination of the Ritz method and the Penalty Function Method is used to relax the admissibility requirement on the coordinate functions. Plates with different type of curved hinge are presented and a natural parametrization is used to describe the mentioned curves. To demonstrate the validity and efficiency of the proposed algorithm, results of a convergence study and some particular cases compared with results obtained by other authors are included. Finally, several numerical examples not previously treated are presented.

## 2. Analysis

Let us consider a rectangular anisotropic plate that in the equilibrium position covers the two-dimensional domain  $G$ , with piecewise boundary  $\partial G$  elastically restrained against rotation and translation. The plate has one arbitrary intermediate curve with hinges elastically restrained against rotation and translation. A parabola and an inclined line will be considered as particular cases, as it is shown in Fig. 1. In order to analyze the transverse displacements of the system under study we suppose that the vertical position of the plate at any time  $t$ , is described by the function  $w^{(k)}(x, y, t) \in G^{(k)}$ , with  $k = 1, 2$ , where  $x = (x_1, x_2) \in \bar{G}$ ,  $\bar{G} = G \cup \partial G$  and that the domain  $G$  is divided by the curve  $\Gamma_c$  into the sub-domains  $G^{(1)}$  and  $G^{(2)}$ , with boundaries  $\partial G_i, i = 1, \dots, 4$ , where  $\partial G_2 = \partial G_2^{(1)} \cup \partial G_2^{(2)}$  and  $\partial G_4 = \partial G_4^{(1)} \cup \partial G_4^{(2)}$  (see Fig. 1).

The rectangular plate has a constant thickness  $h$ , the rotational and translational rigidities of the elastic restraints along the boundary are respectively given by  $r_i$  and  $t_i$ , with  $i = 1, \dots, 4$ . The curve  $\Gamma_c$  has a

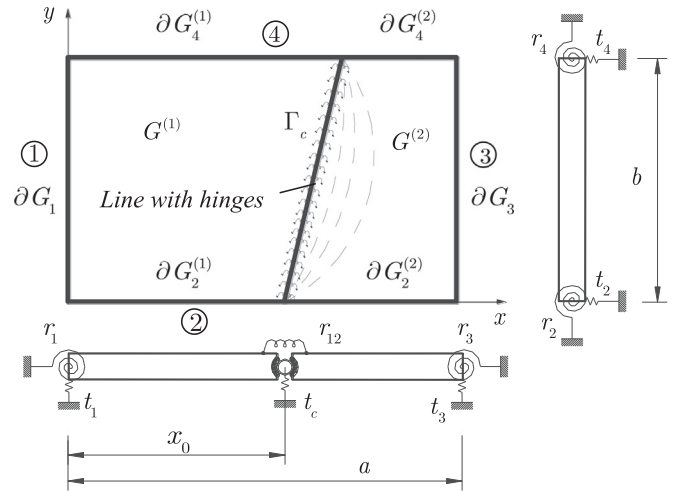


Fig. 1. Mechanical system under study.

rotational elastic restraint  $r_{12}$  that is connected to each subdomain of the plate and it also has a translational restraint  $t_c$  that one end is connected to the curve with hinges and the other end is connected to a fixed point (see Fig. 1).

The mechanical behavior of  $\Gamma_c$  allows the rotation in the direction of its normal vectors  $\vec{n}_c^{(1)}$  and  $\vec{n}_c^{(2)}$  when  $0 \leq r_{12} < \infty$ , and the normal displacement of the plate is continuous along  $\Gamma_c$  (see Fig. 2). Therefore, it is allowed a discontinuity in the slope of the displacement at  $\Gamma_c$ .

When the plate makes free vibrations, its displacement is given by a harmonic function of the time, i.e.

$$w^{(k)}(x, y, t) = W^{(k)}(x, y)\cos(\omega t), \quad k = 1, 2, \quad (1)$$

where  $\omega$  is the radian frequency of the plate and  $W^{(k)}(x, y)$  are the plate displacements amplitude of each subdomain.

Considered the established kinematics and basic assumptions of the classical plate theory, the maximum kinetic energy of the vibrating plate is given by

$$T_{\max} = \frac{\rho h \omega^2}{2} \sum_{k=1}^2 \iint_{G^{(k)}} (W^{(k)}(x, y))^2 dx dy, \quad (2)$$

where  $\rho$  is the mass density of the plate.

The maximum potential energy of the mechanical system is given by

$$U_{\max} = U_{P, \max} + U_{R, \max} + U_{T, \max}, \quad (3)$$

where  $U_{P, \max}$  is the maximal potential energy of the plate bending, that is given by

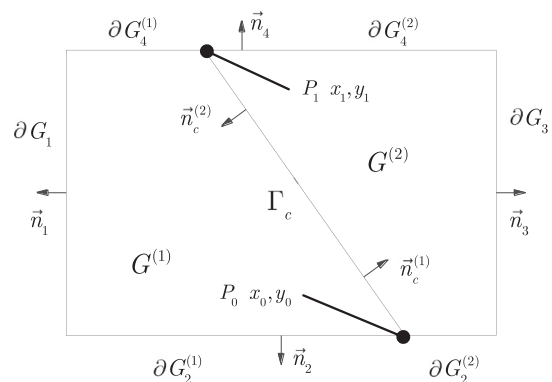


Fig. 2. Mechanical system under study.

$$\begin{aligned}
 U_{P, \max} = & \frac{1}{2} \sum_{k=1}^2 \iint_{G^{(k)}} \left[ D_{11}^{(k)} \left( \frac{\partial^2 W^{(k)}}{\partial x^2} \right)^2 + 2D_{12}^{(k)} \frac{\partial^2 W^{(k)}}{\partial x^2} \frac{\partial^2 W^{(k)}}{\partial y^2} \right. \\
 & + D_{22}^{(k)} \left( \frac{\partial^2 W^{(k)}}{\partial y^2} \right)^2 + 4 \left( D_{16}^{(k)} \frac{\partial^2 W^{(k)}}{\partial x^2} + D_{26}^{(k)} \frac{\partial^2 W^{(k)}}{\partial y^2} \right) \frac{\partial^2 W^{(k)}}{\partial x \partial y} \\
 & \left. + 4D_{66}^{(k)} \left( \frac{\partial^2 W^{(k)}}{\partial x \partial y} \right)^2 \right] dx \, dy, \tag{4}
 \end{aligned}$$

where  $D_{ij}^{(k)}$ ,  $k = 1, 2, i, j = 1, 2, 6$ , are the plate rigidity that takes into account bending, torsion and coupled effects.

The maximum potential energy  $U_{T, \max}$  of the elastic translational restrictions is given by

$$U_{T, \max} = \frac{1}{2} \sum_{i=1}^4 \int_0^{l_i} t_i(W(s))^2 ds + \frac{1}{2} \int_{\Gamma_c} t_c(W(s))^2 ds, \tag{5}$$

where  $s$  is the arc length along the boundary  $\partial G_i, l_i$  is the length of the boundary  $\partial G_i, i = 1, \dots, 4$  and  $W(s)$  is given by

$$W(s) = \begin{cases} W^{(1)}(s) & \forall s \in (\partial G_4^{(1)} \cup \partial G_1 \cup \partial G_2^{(1)}) \\ W^{(2)}(s) & \forall s \in (\partial G_2^{(2)} \cup \partial G_3 \cup \partial G_4^{(2)}), \end{cases} \tag{6}$$

Finally, the maximum potential energy of the rotational restrictions is given by

$$U_{R, \max} = \frac{1}{2} \sum_{i=1}^4 \int_{\Gamma_c} r_i \left( \frac{\partial W}{\partial \vec{n}_i} \right)^2 ds + \frac{1}{2} \int_{\Gamma_c} r_{12} \left( \frac{\partial W^{(1)}}{\partial \vec{n}_c^{(1)}} + \frac{\partial W^{(2)}}{\partial \vec{n}_c^{(2)}} \right)^2 ds, \tag{7}$$

where  $\frac{\partial W}{\partial \vec{n}_i}$  is the directional derivative of  $W$  with respect to the outward normal unit vector  $\vec{n}_i$  to the boundary curve  $\partial G_i, \frac{\partial W^{(k)}}{\partial \vec{n}_c^{(k)}}$  denotes the directional derivatives with respect to the outward normal unit vector  $\vec{n}_c^{(k)}$  to the curve  $\Gamma_c$  when it is considered to be part of the subdomain  $G^{(k)}$  (see Fig. 2).

The values of the outward normal unit vector  $\vec{n}_i$  of the rectangular anisotropic plate are given by (see Fig. 2)

$$\begin{cases} n_{x_1} = -1, & \begin{cases} n_{x_2} = 0, & \begin{cases} n_{x_3} = 1, & \begin{cases} n_{x_4} = 0, \\ n_{y_1} = 0, & \begin{cases} n_{y_2} = -1, & \begin{cases} n_{y_3} = 0, & \begin{cases} n_{y_4} = 1. \end{cases} \end{cases} \end{cases} \end{cases} \end{cases} \end{cases} \end{cases} \tag{8}
 \end{cases}$$

Let us consider that  $n_{x_c}^{(k)}$  and  $n_{y_c}^{(k)}$  are the components of the outward normal unit vector  $\vec{n}_c^{(k)}$ , then Eq. (7) becomes

$$\begin{aligned}
 U_{R, \max} = & \frac{1}{2} \sum_{i=1}^4 \int_{\Gamma_c} r_i \frac{\partial W}{\partial \vec{n}_i} \left( \frac{\partial W}{\partial x} n_{x_i} + \frac{\partial W}{\partial y} n_{y_i} \right) ds + \\
 & + \frac{1}{2} \int_{\Gamma_c} r_{12} \left[ \left( \frac{\partial W^{(1)}}{\partial x} n_{x_c}^{(1)} + \frac{\partial W^{(1)}}{\partial y} n_{y_c}^{(1)} \right) + \left( \frac{\partial W^{(2)}}{\partial x} n_{x_c}^{(2)} + \frac{\partial W^{(2)}}{\partial y} n_{y_c}^{(2)} \right) \right]^2 ds \tag{9}
 \end{aligned}$$

### 3. Combination of The Ritz and Penalty Function Methods

#### 3.1. Problem description

When the Ritz method is applied to a mechanical system, the solution for the governing eigenvalue equation of the plate is obtained by defining the characteristic function depending on the boundary conditions. In the system described in this work, there exists an intermediate condition that requires the continuity of the displacements along the curve with hinges. This transition conditions generate various problems in the construction and rational election of the shape functions. Fortunately it is not necessary to subject the coordinate functions to the natural boundary conditions [31,32]. This concept can be extended to the transition conditions and is particularly true in the

case of a plate with an internal line hinge [21,24].

According to [21,23,24] the only essential transition conditions of the problem under study is that ensures the continuity of transverse displacement along the line hinge and which imposes the analytical condition

$$W^{(1)}(s) - W^{(2)}(s) = 0, \quad \forall s \in \Gamma_c. \tag{10}$$

The constraint condition (10) is added to the energy functional of the problem by means of a suitable penalty parameter [28]. This leads to the following functional:

$$H(W) = \Pi(W) + G(W), \tag{11}$$

where

$$\Pi = U_{\max} - T_{\max}, \tag{12}$$

is the functional of the analyzed mechanical system and

$$G(W) = \frac{K}{2} \int_{\Gamma_c} (W^{(1)}(s) - W^{(2)}(s))^2 ds, \tag{13}$$

is the subsidiary condition, where  $K$  is the penalty parameter [25–28].

Now, the idea is to minimize the functional (11) over the deflection functions which satisfy only the geometrical boundary conditions on the subdomains  $G^{(1)}$  and  $G^{(2)}$ .

#### 3.2. Curvilinear integral along the curve hinge of the transition condition

It is well known that if  $f: \text{im}(\beta) \rightarrow \mathbb{R}$  a continuous function defined on the image  $\Gamma$  of a piecewise smooth path  $\beta: [a', b'] \rightarrow \Gamma$ , the curvilinear integral of  $f$  along  $\Gamma$  is given by [33]

$$\int_{\Gamma} f(x, y) ds = \int_{a'}^{b'} (f \circ \beta)(r) \|\beta'(r)\| dr, \tag{14}$$

where  $(f \circ \beta)(r) = f(\beta(r))$  and the norm  $\|\beta'(r)\|$  is given by  $\sqrt{\beta_1'^2(r) + \beta_2'^2(r)}$ , where  $\beta'(r) = d\beta/dr$ . The vectors  $\pm(\beta_2'(r), -\beta_1'(r))$  are normal to  $\Gamma$  at  $\beta(r)$ . In the case of a regular point  $r$ , the unit normal vector to the curve is given by

$$\vec{n}_c^{(k)} = (-1)^{(k+1)} \frac{(\beta_2'(r), -\beta_1'(r))}{\|\beta'(r)\|}. \tag{15}$$

where  $k = 1, 2$ .

#### 3.3. Particular case: Internal hinges located along a straight line

In the case of a straight line represented with the equation  $y = mx + n$ , that passes through two different points  $P_0(x_0, y_0)$  and  $P_1(x_1, y_1)$ , its parametric form is given by (see Fig. 2)

$$\beta(r) = \left( \frac{r - n}{m}, r \right), \quad \beta: [y_0, y_1] \rightarrow \Gamma_c. \tag{16}$$

Taking into account that in this particular case  $\|\frac{d\beta}{dr}\| = \|(1/m, 1)\| = \sqrt{1 + m^2}/m$ , and using (16), the curvilinear integral (13) when  $r$  is substituted by  $y$  is given by

$$\frac{K}{2} \int_{y_0}^{y_1} (W^{(1)}((y - n)/m, y) - W^{(2)}((y - n)/m, y))^2 \sqrt{1 + m^2}/m dy, \tag{17}$$

where  $y_0 = 0$  and  $y_1 = b$ .

#### 3.4. Particular case: internal hinges located along a parabolic curve with its edge parallel to y-axis

The quadratic equation that represents the curve  $\Gamma_c$  is given by

$$y = a_1 x^2 + a_2 x + a_3, \tag{18}$$

where  $a_1 = \frac{1}{4p}, a_2 = -\frac{f}{2p}, a_3 = \frac{f^2}{4p} + h, (f, h)$  is the vertex point of the parabola and  $p$  is the distance from the vertex point to the focus. Eq.

(18) could be rewritten as

$$(x - f)^2 = 4p(y - h). \tag{19}$$

The parametric form of (19) is

$$\beta(r) = (2\sqrt{p(r - h)} + f, r), \quad \beta: [y_0, y_1] \rightarrow \Gamma_c. \tag{20}$$

Taking into account Eq. (19) and

$$\left\| \frac{d\beta}{dr} \right\| = \left\| \left( \sqrt{\frac{p}{r - h}}, 1 \right) \right\| = \sqrt{1 + \frac{p}{r - h}}, \tag{21}$$

The curvilinear integral of Eq. (13) when  $r$  is substituted by  $y$  is

$$\begin{aligned} & \frac{\kappa}{2} \int_{y_0}^{y_1} [W^{(1)}(2\sqrt{p(y - h)} + f, y) \\ & - W^{(2)}(2\sqrt{p(y - h)} + f, y)]^2 (\sqrt{1 + p/(y - h)}) dy. \end{aligned} \tag{22}$$

### 3.5. Particular case: Internal hinges located along a parabolic curve with its edge parallel to $x$ -axis

The quadratic equation that represents the curve  $\Gamma_c$  is given by

$$x = a_1 y^2 + a_2 y + a_3, \tag{23}$$

where  $a_1 = \frac{1}{4p}, a_2 = -\frac{h}{2p}, a_3 = \frac{h^2}{4p} + f$ , and Eq. (23) could be rewritten as

$$(y - h)^2 = 4p(x - f). \tag{24}$$

The parametric form of (24) is

$$\beta(r) = \left( \frac{(r - h)^2}{4p} + f, r \right), \quad \beta: [y_0, y_1] \rightarrow \Gamma_c. \tag{25}$$

Taking into account Eq. (24) and

$$\left\| \frac{d\beta}{dr} \right\| = \left\| \left( \frac{r - h}{2p}, 1 \right) \right\| = \sqrt{1 + \frac{(r - h)^2}{4p^2}}, \tag{26}$$

The curvilinear integral of Eq. (13) when  $r$  is substituted by  $y$  is

$$\begin{aligned} & \frac{\kappa}{2} \int_{y_0}^{y_1} [W^{(1)}((y - h)^2/4p + f, y) \\ & - W^{(2)}((y - h)^2/4p + f, y)]^2 \sqrt{1 + (y - h)^2/4p^2} dy. \end{aligned} \tag{27}$$

### 3.6. Approximating functions

In the present paper the transverse deflection of the rectangular plate is represented by means of

$$W^{(k)}(x, y) = \sum_{i=1}^M \sum_{j=1}^N c_{ij}^{(k)} p_i^{(k)}(x) q_j^{(k)}(y) \text{ if } (x, y) \in \bar{G}^{(k)}, \quad k = 1, 2, \tag{28}$$

where  $c_{ij}^{(1)}$  and  $c_{ij}^{(2)}$  are unknown coefficients,  $\{p_i^{(k)}(x)\}, \{q_j^{(k)}(y)\}, k = 1, 2$  are sets of polynomial functions generated automatically from base polynomials that satisfies the geometrical boundary conditions of each subdomain.

The higher members of the described sets are automatically generated using the following procedure:

$$p_i^{(k)}(x) = p_1^{(k)}(x)x^{i-1}, \quad i = 2, \dots, M, \quad k = 1, 2, \tag{29}$$

$$q_j^{(k)}(y) = q_1^{(k)}(y)y^{j-1}, \quad j = 2, \dots, N, \quad k = 1, 2. \tag{30}$$

where  $p_1^{(k)}(x)$  and  $q_1^{(k)}(y)$  are the first polynomials that satisfy the geometrical boundary conditions.

### 3.7. The eigenvalue equation

If we consider the energy functional (11) and it is introduced the energy expressions (5) and (7), the application of the Ritz method in conjunction with the penalty function method requires that the condition of the stationary functional must satisfy [29]

$$\delta H(W; V) = 0, \tag{31}$$

where  $V$  denote the admissible directions for  $W$ .

The condition (31) leads to the variational formulation [29]

$$\delta H(W; V) = 0 \Rightarrow \delta \Pi(W) + \delta G(W) = 0, \tag{32}$$

Substituting Eq. (28) into Eq. (32), a governing eigenvalue problem is obtained, which is

$$([K] - \omega^2 [M])\{c\} = \{0\}, \tag{33}$$

where the matrix  $[K]$  and  $[M]$  are given by:

$$[K] = \begin{bmatrix} [K^{(1,1)}] & [K^{(1,2)}] \\ [K^{(2,1)}] & [K^{(2,2)}] \end{bmatrix}, \tag{34}$$

$$[M] = \begin{bmatrix} [M^{(1,1)}] & [0] \\ [0] & [M^{(2,2)}] \end{bmatrix}. \tag{35}$$

The expressions of the elements of these matrixes are given in Appendix A.

## 4. Numerical results

The terminology to be used throughout the numerical results for describing the boundary conditions of the plate considered will now be introduced. In all tables and figures, the symbol F, S and C denote free, simply supported and clamped edges and for example in the designation CSFS, the first symbol indicates the boundary condition at  $x = 0$ , the second at  $y = 0$ , the third at  $x = a$ , and the fourth at  $y = b$ .

In order to establish the accuracy and applicability of the approach developed and discussed in the previous sections, numerical results were computed for a number of plate problems for which some particular cases were compared with ones available in the literature. Additionally, new numerical results were generated for rectangular plates with different curve hinge cases and locations and different boundary conditions. All calculations have been performed taking  $N = M = 7$ , Poisson's ratio  $\mu = 0.3$  and  $R_{12} = 0$ , unless otherwise specified.

In the case of isotropic plate, results of the values of the frequency parameter  $\Omega = \omega b^2 \sqrt{\rho h / D}$ , are presented. The isotropy is characterized by

$D_{11} = D_{22} = D, D_{16} = D_{26} = 0, D_{12} = \mu D, D_{66} = 0.5(1 - \mu)D$ , where  $D$  denotes the flexural rigidity of the isotropic plate.

The position of the hinges along a straight line is given by the points  $P_0(x_0, 0)$  and  $P_1(x_1, b)$  as shown in Fig. 2. When the hinges are distributed along a parabola, it is given by its edge, vertex  $(f, h)$  and the distance from the vertex to the focus  $p$ .

Fig. 3 shows a convergence study of the first six values of  $\Omega/\hat{\Omega}$  for a SSSS isotropic square plate with free internal hinges distributed along a straight line with  $x_0 = 0.4$  and  $x_1 = 0.8$ , where  $\hat{\Omega}$  are the values of  $\Omega$  when  $N = M = 11$ . The values of  $\hat{\Omega}$  from mode 1–6 are 15.47, 44.28, 46.06, 74.11, 87.33, 94.66. Results of the convergence study shown that a value of  $N = M = 7$  is enough for a good computation of the frequency parameter.

Fig. 4 shows a convergence study of the first six values of  $\Omega/\hat{\Omega}$  for a SSSS isotropic square plate with free internal hinges distributed along a parabola with vertical edge,  $f = -0.2, h = -0.2$ , and  $p = 0.2$ . The values of  $\hat{\Omega}$  from mode 1–6 are 14.57, 43.37, 48.18, 68.94, 87.64, 94.14. Results shown that in this case a value of  $N = M = 9$  should be used for a correct computation of the frequency parameter.

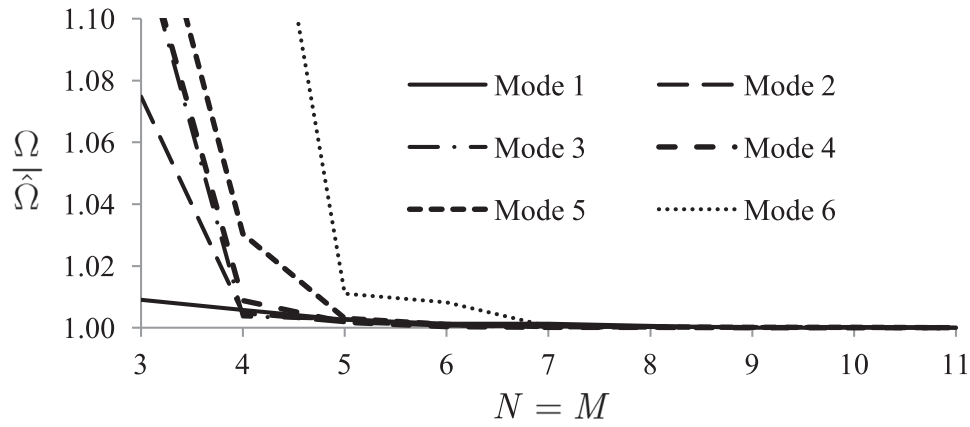


Fig. 3. Convergence study of the first six values of  $\Omega/\hat{\Omega}$  for a SSSS isotropic square plate with free internal hinges distributed along a straight line with  $x_0 = 0.4$  and  $x_1 = 0.8$ .

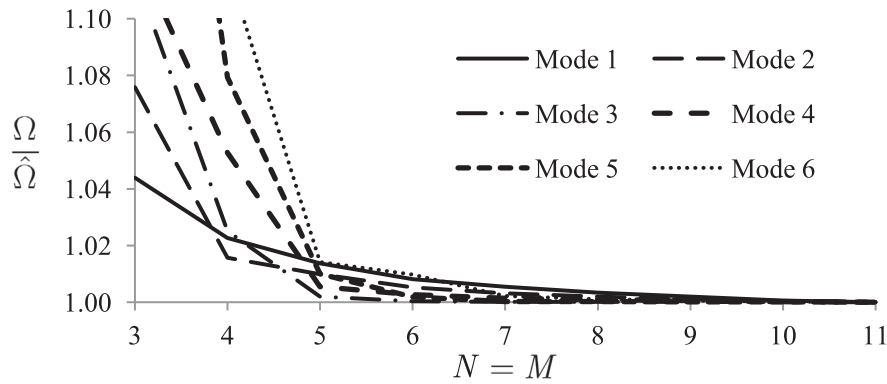


Fig. 4. Convergence study of the first six values of  $\Omega/\hat{\Omega}$  for a SSSS isotropic square plate with free internal hinges distributed along a parabola with vertical edge with  $f = -0.2, h = -0.2$ , and  $p = 0.2$ .

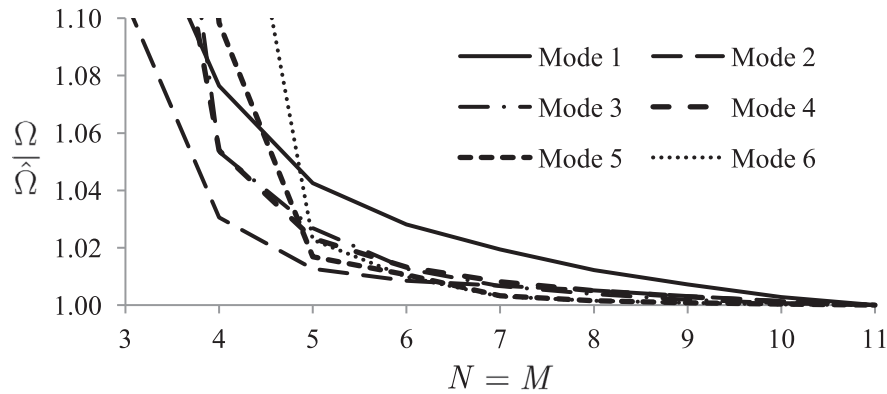


Fig. 5. Convergence study of the first six values of  $\Omega/\hat{\Omega}$  for a SSSS isotropic square plate with free internal hinges distributed along a parabola with horizontal edge with  $f = 0.1, h = 0.0$ , and  $p = 0.3$ .

Fig. 5 shows a convergence study of the first six values of  $\Omega/\hat{\Omega}$  for a SSSS isotropic square plate with free internal hinges distributed along a parabola with horizontal edge,  $f = 0.1, h = 0.0$ , and  $p = 0.3$ . The values of  $\hat{\Omega}$  from mode 1–6 are 13.88, 40.95, 41.74, 71.00, 87.08, 92.75. Results shown that a value of  $N = M = 10$  should be used for a correct computation of the frequency parameter.

Table 1 gives the first six values of the frequency parameter  $\Omega = \omega b^2 \sqrt{\rho h / D}$  and their modal shapes contour lines of a SSSS isotropic square plate with free internal hinges distributed along a straight line with  $x_0 = 0.5$ , for different values of  $x_1$ . When  $x_1 = 0.5$ , the values were compared with the ones presented in [21]. The modal contour lines shown correspond to  $x_1 = 0.1, 0.5$  and  $0.99$ . Results were computed with

$N = M = 9$ .

Table 2 gives the first six values of the frequency parameter  $\Omega = \omega b^2 \sqrt{\rho h / D}$ , of a SSSS isotropic square plate with a rotational elastic restriction  $r_{12} = RD_{11}^{(1)}$ , for different values of  $R$  along a straight line with  $x_0 = 0.1$  and  $x_1 = 0.9$ . Results were computed taking into account  $N = M = 9$ . When  $R = \infty$ , the values of the frequency parameter are compared with the ones obtained by Grossi and Raffo [23]. It is observed a very good agreement between the results of present analysis and those of [23].

Table 3 gives the first six values of the frequency parameter  $\Omega$  for a SSSS isotropic square plate with free internal hinges distributed along a parabola with vertical edge, with  $f = 0.0, h = -0.01$ , for different values



**Table 1**

First six values of the frequency parameter  $\Omega$  and their modal shapes contour lines of a SSSS isotropic square plate with free internal hinges distributed along a straight line with  $x_0 = 0.5$ , for different values of  $x_1$ .

Modal sequence						
$x_1$	1	2	3	4	5	6
0.1	15.9710	39.1351	46.4099	71.8047	93.5841	95.7653
0.3	16.0818	44.6786	46.6403	75.5342	88.0002	95.8243
0.5	16.1348	46.7381	49.3480	75.2834	78.9568	96.0406
[21]	16.1348	46.7381	49.3480	75.2834	78.9568	96.0406
0.6	16.1204	46.6676	47.8493	76.7183	80.4007	95.9908
0.8	16.0307	41.6466	46.4867	73.5519	94.7940	95.7897
0.99	15.7385	37.3018	46.3957	70.8704	88.4590	95.5711

**Table 2**

First six values of the frequency parameter  $\Omega = \omega b^2 \sqrt{\rho h / D}$ , of a SSSS isotropic square plate with a rotational elastic restriction  $\eta_2 = RD_{11}^{(1)}$ , along a straight line with  $x_0 = 0.1$  and  $x_1 = 0.9$ .

$R$	Modal sequence					
	1	2	3	4	5	6
0	13.3178	40.6105	49.3477	64.1727	85.3276	97.9660
0.01	13.3497	40.6362	49.3477	64.2166	85.3572	97.9672
0.1	13.6223	40.8608	49.3477	64.6007	85.6175	97.9785
1	15.4408	42.6023	49.3478	67.5888	87.7717	98.0750
10	18.6467	47.1419	49.3479	75.3087	94.6364	98.4325
100	19.6089	49.0609	49.3480	78.4884	98.1407	98.6571
1000	19.7258	49.3182	49.3480	78.9084	98.6383	98.6920
10000	19.7379	49.3450	49.3480	78.9520	98.6903	98.6957
$\infty$	19.7392	49.3480	49.3480	78.9568	98.6961	98.6961
[23]	19.7392	49.3480	49.3480	78.9568	98.6960	98.6960

of  $p$ . It is observed that as the value of  $p$  diminishes, results tends to the ones which corresponds to a SSSS isotropic rectangular plate without internal hinges.

Fig. 6 gives the first ten values of the frequency parameter

$\Omega = \omega b^2 \sqrt{\rho h / D_{11}^{(1)}}$  and their modal shapes contour lines of an anisotropic square plate with free internal hinges distributed along a parabola given by its vertical edge, its vertex  $(-0.1, -0.1)$  and  $p = 0.1$ . The boundary conditions of the plate are clamped at  $x = 0$ , free at  $y = 0$ , free at  $x = a$ , and at  $y = b$  the plate is free at  $\partial G_4^{(1)}$  and simply supported at  $\partial G_3^{(2)}$ . The anisotropy of  $G^{(1)}$  is characterized by  $D_{22}^{(1)} / D_{11}^{(1)} = 0.2, D_{12}^{(1)} / D_{11}^{(1)} = 0.8, D_{16}^{(1)} / D_{11}^{(1)} = -0.2, D_{26}^{(1)} / D_{11}^{(1)} = -0.8$  and  $D_{66}^{(1)} / D_{11}^{(1)} = 0.4$ , the anisotropy of  $G^{(2)}$  is characterized by  $D_{22}^{(2)} / D_{11}^{(2)} = 1.0, D_{12}^{(2)} / D_{11}^{(2)} = 0.1, D_{16}^{(2)} / D_{11}^{(2)} = -0.025, D_{26}^{(2)} / D_{11}^{(2)} = -0.1$  and  $D_{66}^{(2)} / D_{11}^{(2)} = 0.05$ .

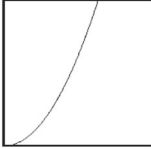
Fig. 7 gives the first six values of the frequency parameter  $\Omega = \omega b^2 \sqrt{\rho h / D}$  and their modal shapes contour lines of a SSSS isotropic square plate with free internal hinges distributed along a parabola with horizontal edge, for  $f = 0.1, h = 0.0, p = 0.3$  and  $f = 0.2, h = 0.0, p = 0.1$ .

Fig. 8 gives the first six values of the frequency parameter  $\Omega = \omega b^2 \sqrt{\rho h / D_{11}^{(1)}}$ , and their modal shapes contour lines of a SSSS rectangular plate with  $a/b = 2$ , and a free internal line hinge distributed along a straight line with  $\bar{x}_0 = x_0/a = 0.2$  and  $\bar{x}_1 = x_1/a = 0.8$ . The sub-domain  $G^{(1)}$  is made of an anisotropic material and  $G^{(2)}$  is made of an isotropic material. The anisotropy of  $G^{(1)}$  is characterized by  $D_{22}^{(1)} / D_{11}^{(1)} = 0.2130195, D_{12}^{(1)} / D_{11}^{(1)} = 0.3245569, D_{16}^{(1)} / D_{11}^{(1)} = 0.5120546, D_{26}^{(1)} / D_{11}^{(1)} = 0.1694905$  and  $D_{66}^{(1)} / D_{11}^{(1)} = 0.3387559$ . Results were computed


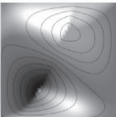
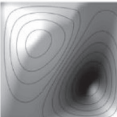
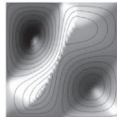
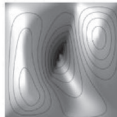
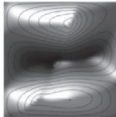
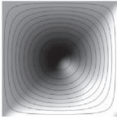
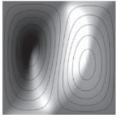
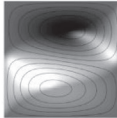
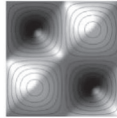
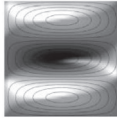
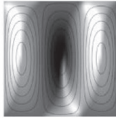
**Table 3**

First six values of the frequency parameter  $\Omega$  for a SSSS isotropic square plate with free internal hinges distributed along a parabola with vertical edge, with  $f = 0.0, h = -0.01$ , for different values of  $p$ . Modal shapes shown corresponds to  $p = 0.1$  and  $p = 10^{-6}$ .


Curve shape:



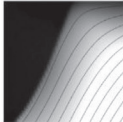
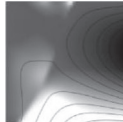
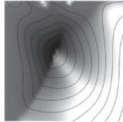
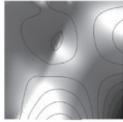
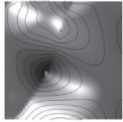
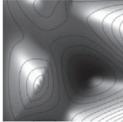
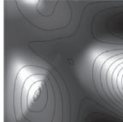
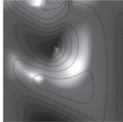
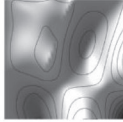
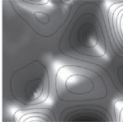
$p = \blacksquare$

Modal Sequence						
$p$	1	2	3	4	5	6
0.1	14.8235	43.8190	48.1511	70.6121	85.0942	94.3055
						
$10^{-2}$	17.9215	35.8688	48.5537	71.8965	75.9296	97.9381
$10^{-3}$	19.2939	42.5214	49.2166	73.6289	77.8819	98.6021
$10^{-4}$	19.6321	47.5621	49.3209	78.4605	89.0595	98.6938
$10^{-5}$	19.7153	48.9459	49.3425	78.8389	97.6015	98.7110
$10^{-6}$	19.7355	49.2803	49.3475	78.9265	98.7147	99.6933
						

Curve shape:



Modal Sequence

1	2	3	4	5
				
1.9664	16.5970	19.5587	25.1793	39.4813
6	7	8	9	10
				
49.7111	53.5146	62.2389	67.1879	85.1562

**Fig. 6.** First ten values of the frequency parameter  $\Omega = \omega b^2 \sqrt{\rho h / D_{11}^{(1)}}$  and their modal shapes contour lines of an anisotropic square plate with free internal hinges distributed along a parabola with vertical edge, with  $f = -0.1, h = -0.1$  and  $p = 0.1$ . The boundary conditions of the plate are clamped at  $x = 0$ , free at  $y = 0$ , free at  $x = a$ , and at  $y = b$  the plate is free at  $\partial G_4^{(1)}$  and simply supported at  $\partial G_4^{(2)}$ .

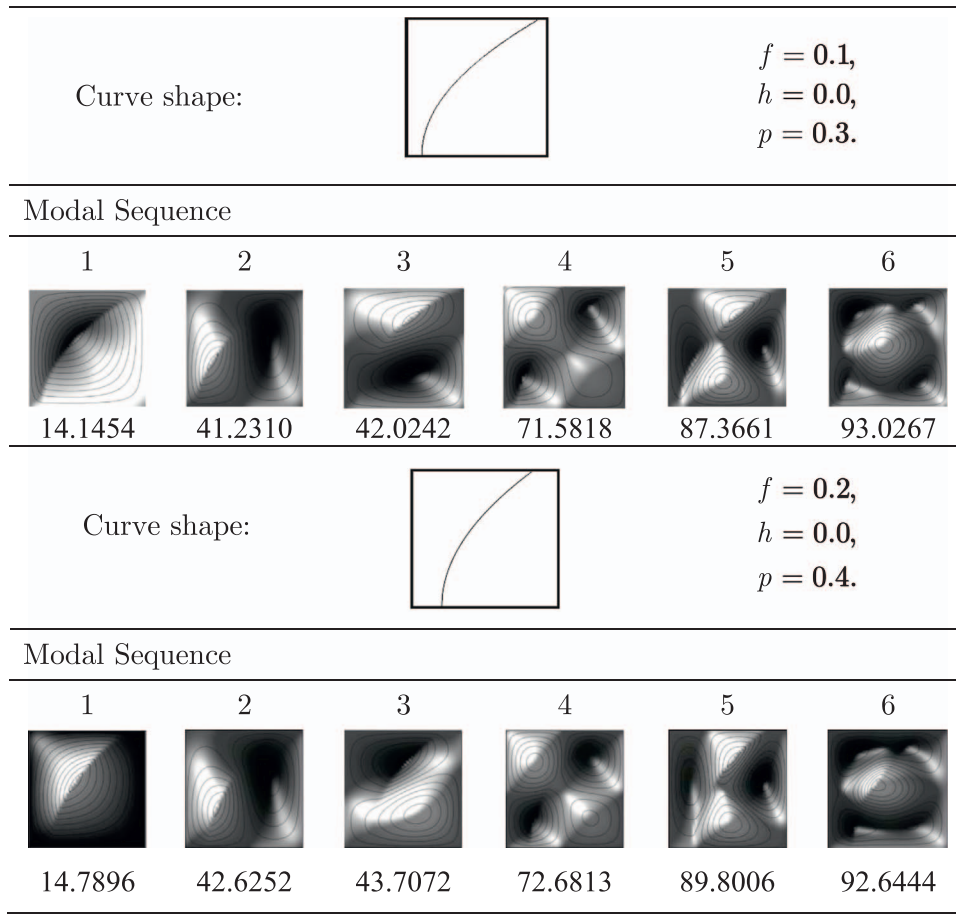


Fig. 7. First six values of the frequency parameter  $\Omega = \omega b^2 \sqrt{\rho h D}$  and their modal shapes contour lines of a SSSS isotropic square plate with free internal hinges distributed along a parabola with horizontal edge with  $f = 0.1, h = 0.0, p = 0.3$  and  $f = 0.2, h = 0.0, p = 0.4$ .

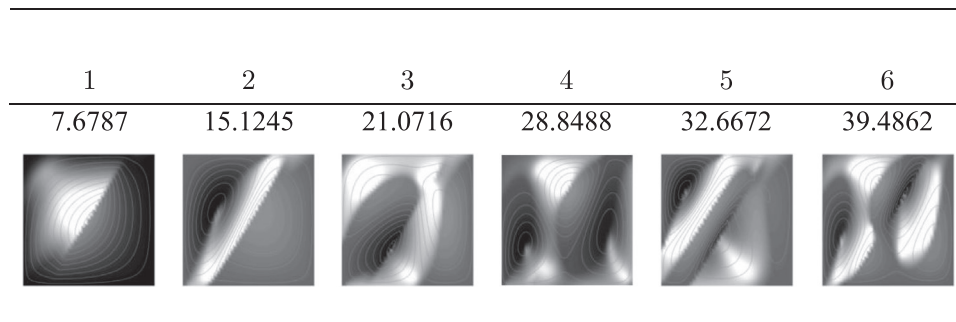


Fig. 8. First six values of the frequency parameter  $\Omega$  and their modal shapes contour lines of a SSSS rectangular plate with a free internal line hinge distributed along a straight line with  $\bar{x}_0 = x_0/a = 0.2, \bar{x}_1 = x_1/a = 0.8$ , and  $a/b = 2$ . The sub-domain  $G^{(1)}$  is made of an anisotropic material and  $G^{(2)}$  is made of an isotropic material.

taking into account  $N = M = 9$ .

Table 4 gives the first six values of the frequency parameter  $\Omega = \omega b^2 \sqrt{\rho h D_{11}^{(1)}}$ , of a CSRF isotropic square plate, where R boundary condition means that at  $x = a$ , the plate is simply supported and it also have a rotational elastic restriction  $r_3 = RD_{11}^{(1)}/a$ . The plate also have a free internal hinges distributed along a straight line with  $x_0 = 0.1$  and  $x_1 = 0.7$ .

### 5. Concluding remarks

In this paper, an approach to the solution of the natural vibration problems of anisotropic plates with an internal curved line hinge, by a direct variational method, has been presented. The presence of an internal curve with hinges constitutes a complicating effect to obtain satisfactory numerical results.

The governing differential equation has been derived based on classical plate theory. The analytical solution was obtained based on a combination of the Ritz method and the penalty function method. The penalty method was used to connect the modes of each subdomain as admissible forms for the system, leading to a general formulation. Sets of parametric studies have been performed in order to examine the accuracy and efficiency of the proposed methodology. Finally, the influence of the internal curved hinge and its location on the vibration behaviour has been analysed. Tables and figures are presented for plates with different characteristics.

### Acknowledgments

This paper has been partially sponsored by the UTN, Argentina project 3487 and CIUNSA, Argentina project 2153.



**Appendix A**

The elements of the rigidity matrix  $[K]$  and mass matrix  $[M]$  are given by

$$\begin{aligned}
 K_{ijkl}^{(1,1)} = & \int_0^b \int_0^{\beta^1(y)} [D_{11}^{(1)} P_{ij}^{(1)(2,0)} Q_{kl}^{(1)(2,0)} \\
 & + D_{12}^{(1)} (P_{ij}^{(1)(0,2)} Q_{kl}^{(1)(2,0)} + P_{ij}^{(1)(2,0)} Q_{kl}^{(1)(0,2)}) \\
 & + D_{22}^{(1)} P_{ij}^{(1)(0,2)} Q_{kl}^{(1)(0,2)} + 2D_{16}^{(1)} (P_{ij}^{(1)(1,1)} Q_{kl}^{(1)(2,0)} + P_{ij}^{(1)(2,0)} Q_{kl}^{(1)(1,1)}) \\
 & + 2D_{26}^{(1)} (P_{ij}^{(1)(1,1)} Q_{kl}^{(1)(0,2)} + P_{ij}^{(1)(0,2)} Q_{kl}^{(1)(1,1)}) + 4D_{66}^{(1)} P_{ij}^{(1)(1,1)} Q_{kl}^{(1)(1,1)}] dx dy \\
 & + r_1 \int_0^b P_{ij}^{(1)(1,0)} Q_{kl}^{(1)(1,0)} \Big|_{x=0} dx + t_1 \int_0^b P_{ij}^{(1)(0,0)} Q_{kl}^{(1)(0,0)} \Big|_{x=0} dy \\
 & + r_2 \int_0^{x_0} P_{ij}^{(1)(0,1)} Q_{kl}^{(1)(0,1)} \Big|_{y=0} dx + t_2 \int_0^{x_0} P_{ij}^{(1)(0,0)} Q_{kl}^{(1)(0,0)} \Big|_{y=0} dx \\
 & + r_4 \int_0^{x_1} P_{ij}^{(1)(0,1)} Q_{kl}^{(1)(0,1)} \Big|_{y=b} dx + t_4 \int_0^{x_1} P_{ij}^{(1)(0,0)} Q_{kl}^{(1)(0,0)} \Big|_{y=b} dx \\
 & + r_{12} \int_0^b \left[ \left( P_{ij}^{(1)(1,0)} n_{x_c}^{(1)} + P_{ij}^{(1)(0,1)} n_{x_c}^{(1)} \right) \left( Q_{kl}^{(1)(1,0)} n_{x_c}^{(1)} + Q_{kl}^{(1)(0,1)} n_{x_c}^{(1)} \right) \right] \Big|_{x=\beta^1(y)} \left\| \frac{d\beta}{dr} \right\| dy \\
 & + t_c \int_0^b P_{ij}^{(1)(0,0)} Q_{kl}^{(1)(0,0)} \Big|_{x=\beta^1(y)} \left\| \frac{d\beta}{dr} \right\| dy + K \int_0^b [P_{ij}^{(1)(0,0)} Q_{kl}^{(1)(0,0)}] \Big|_{x=\beta^1(y)} \left\| \frac{d\beta}{dr} \right\| dy,
 \end{aligned}$$

$$\begin{aligned}
 K_{ijkl}^{(1,2)} = & r_{12} \int_0^b \left[ \left( P_{ij}^{(1)(1,0)} n_{x_c}^{(1)} + P_{ij}^{(1)(0,1)} n_{x_c}^{(1)} \right) \left( Q_{kl}^{(2)(1,0)} n_{x_c}^{(2)} + Q_{kl}^{(2)(0,1)} n_{x_c}^{(2)} \right) \right] \Big|_{x=\beta^1(y)} \left\| \frac{d\beta}{dr} \right\| dy \\
 & - K \int_0^b [P_{ij}^{(1)(0,0)} Q_{kl}^{(2)(0,0)}] \Big|_{x=\beta^1(y)} \left\| \frac{d\beta}{dr} \right\| dy,
 \end{aligned}$$

$$\begin{aligned}
 K_{ijkl}^{(2,1)} = & r_{12} \int_0^b \left[ \left( P_{ij}^{(2)(1,0)} n_{x_c}^{(2)} + P_{ij}^{(2)(0,1)} n_{x_c}^{(2)} \right) \left( Q_{kl}^{(1)(1,0)} n_{x_c}^{(1)} + Q_{kl}^{(1)(0,1)} n_{x_c}^{(1)} \right) \right] \Big|_{x=\beta^1(y)} \left\| \frac{d\beta}{dr} \right\| dy \\
 & - K \int_0^b [P_{ij}^{(2)(0,0)} Q_{kl}^{(1)(0,0)}] \Big|_{x=\beta^1(y)} \left\| \frac{d\beta}{dr} \right\| dy,
 \end{aligned}$$

$$\begin{aligned}
 K_{ijkl}^{(2,2)} = & \int_0^b \int_0^{\beta^1(y)} [D_{11}^{(2)} P_{ij}^{(2)(2,0)} Q_{kl}^{(2)(2,0)} \\
 & + D_{12}^{(2)} (P_{ij}^{(2)(0,2)} Q_{kl}^{(2)(2,0)} + P_{ij}^{(2)(2,0)} Q_{kl}^{(2)(0,2)}) \\
 & + D_{22}^{(2)} P_{ij}^{(2)(0,2)} Q_{kl}^{(2)(0,2)} + 2D_{16}^{(2)} (P_{ij}^{(2)(1,1)} Q_{kl}^{(2)(2,0)} + P_{ij}^{(2)(2,0)} Q_{kl}^{(2)(1,1)}) \\
 & + 2D_{26}^{(2)} (P_{ij}^{(2)(1,1)} Q_{kl}^{(2)(0,2)} + P_{ij}^{(2)(0,2)} Q_{kl}^{(2)(1,1)}) + 4D_{66}^{(2)} P_{ij}^{(2)(1,1)} Q_{kl}^{(2)(1,1)}] dx dy \\
 & + r_2 \int_{x_0}^a P_{ij}^{(2)(0,1)} Q_{kl}^{(2)(0,1)} \Big|_{y=0} dx + t_2 \int_{x_0}^a P_{ij}^{(2)(0,0)} Q_{kl}^{(2)(0,0)} \Big|_{y=0} dx \\
 & + r_3 \int_0^b P_{ij}^{(2)(1,0)} Q_{kl}^{(2)(1,0)} \Big|_{x=a} dy + t_3 \int_0^b P_{ij}^{(2)(0,0)} Q_{kl}^{(2)(0,0)} \Big|_{x=a} dy \\
 & + r_4 \int_{x_1}^a P_{ij}^{(2)(0,1)} Q_{kl}^{(2)(0,1)} \Big|_{y=b} dx + t_4 \int_{x_1}^a P_{ij}^{(2)(0,0)} Q_{kl}^{(2)(0,0)} \Big|_{y=b} dx \\
 & + r_{12} \int_0^b \left[ \left( P_{ij}^{(2)(1,0)} n_{x_c}^{(2)} + P_{ij}^{(2)(0,1)} n_{x_c}^{(2)} \right) \left( Q_{kl}^{(2)(1,0)} n_{x_c}^{(2)} + Q_{kl}^{(2)(0,1)} n_{x_c}^{(2)} \right) \right] \Big|_{x=\beta^1(y)} \left\| \frac{d\beta}{dr} \right\| dy \\
 & + K \int_0^b [P_{ij}^{(2)(0,0)} Q_{kl}^{(2)(0,0)}] \Big|_{x=\beta^1(y)} \left\| \frac{d\beta}{dr} \right\| dy,
 \end{aligned}$$

$$M_{ijkl}^{(1)} = \int_0^b \int_0^{\beta^1(y)} P_{ij}^{(1)(0,0)} Q_{kl}^{(1)(0,0)} dx dy,$$

$$M_{ijkl}^{(2)} = \int_0^b \int_{\beta^1(y)}^a P_{ij}^{(2)(0,0)} Q_{kl}^{(2)(0,0)} dx dy,$$

where

$$P_{ij}^{(\alpha)(r,s)} = \frac{\partial^r P_i^{(\alpha)}(x)}{\partial x^r} \frac{\partial^s q_j^{(\alpha)}(y)}{\partial y^s},$$

$$Q_{kl}^{(\alpha)(r,s)} = \frac{\partial^r p_k^{(\alpha)}(x)}{\partial x^r} \frac{\partial^s q_l^{(\alpha)}(y)}{\partial y^s},$$

$i = 1, \dots, N, j = 1, \dots, M, k = 1, \dots, N$ , and  $l = 1, \dots, M$ . In case of null  $r$  or  $s$  it is assumed that the corresponding derivative is equal to 1. The function  $\beta^l(y)$  is obtained when the value  $r$  is substituted with  $y$ .

## References

- [1] Leissa AW. *Vibration of Plates*. Washington D.C: NASA SP-160; 1969.
- [2] Blevins RD. *Formulas for Natural Frequency and Mode Shape*. Malabar, Florida: Krieger Publishing Company; 1993.
- [3] Gorman DJ. *Free Vibration Analysis of Plates*. New York: Elsevier; 1982.
- [4] Timoshenko S, Woinowsky-Krieger S. *Theory of Plates and Shells*. New York: Mc Graw Hill; 1959.
- [5] Reddy JN. *Mechanics of Laminated Composite Plates and Shells: Theory and Analysis*, 2nd. ed.. Boca Raton, Florida: CRC Press; 2004.
- [6] Leissa AW. The free vibration of rectangular plates. *J Sound Vib* 1973;31:257–93.
- [7] Leissa AW. Recent research in plate vibrations, 1973–1976: complicating effects. *Shock Vib Dig* 1978;10(12):21–35.
- [8] Fan SC, Cheung YK. Flexural free vibrations of rectangular plates with complex support conditions. *J Sound Vib* 1984;31:81–94.
- [9] Kim CS, Dickinson SM. The flexural vibration of rectangular plates with point support. *J Sound Vib* 1987;117:249–61.
- [10] Liew KM, Liu FL. Effects of arbitrarily distributed elastic point constraints on vibrational behavior of rectangular plates. *J Sound Vib* 1994;174:23–36.
- [11] Zhou D. Vibration point-supported rectangular plates with variable thickness using a set of static tapered beam functions. *Int J Mech Sci* 2002;44:149–64.
- [12] Kim CS, Dickinson SM. The flexural vibration of line supported rectangular plate systems. *J Sound Vib* 1987;114:129–42.
- [13] Zhou D, Cheung YK. Free vibration of line supported rectangular plates using a set of static beam functions. *J Sound Vib* 1999;223:231–45.
- [14] Xiang Y, Zhao YB, Wei GW. Levy solutions for vibration of multi-span rectangular plates. *Int J Mech Sci* 2002;44:1195–218.
- [15] Yuan J, Dickinson SM. The flexural vibration of rectangular plate systems approached by using artificial springs in the Rayleigh–Ritz method. *J Sound Vib* 1992;159:39–55.
- [16] Li TY, Liu JX, Zhang T. Vibrational power flow characteristics of circular plate structures with peripheral surface crack. *J Sound Vib* 2004;276:1081–91.
- [17] Wang CM, Xiang Y, Wang CY. Buckling and vibration of plates with an internal line hinge via the Ritz method. in: *Proceedings of the First Asian-Pacific Congress on Computational Mechanics*; 2001, p. 1663-1672
- [18] Gupta PR, Reddy JN. Buckling and vibrations of orthotropic plates with an internal line hinge. *Int J Struct Stab Dyn* 2002;2:457–86.
- [19] Xiang Y, Reddy JN. Natural vibration of rectangular plates with an internal line hinge using the first order shear deformation plate theory. *J Sound Vib* 2003;263:285–97.
- [20] Huang M, Ma XQ, Sakiyama T, Matsuda H, Morita C. Natural vibration study on rectangular plates with a line hinge and various boundary conditions. *J Sound Vib* 2009;322:227–40.
- [21] Quintana MV, Grossi RO. Free vibrations of a generally restrained rectangular plate with an internal line hinge. *Appl Acoust* 2012;73:356–65.
- [22] Grossi RO. Boundary value problems for anisotropic plates with internal line hinges. *Acta Mech* 2012;223:125–44.
- [23] Grossi RO, Raffo JL. Natural vibrations of anisotropic plates with several internal line hinges. *Acta Mech* 2013;224(11):2677–97.
- [24] Quintana MV, Grossi RO. Free vibrations of a trapezoidal plate with an internal line hinge. *Sci World J* 2014;10, [ID 252084, 2014].
- [25] Ilanko S. Penalty methods for finding eigenvalues of continuous systems: emerging challenges and opportunities. *Comput Struct* 2012;104–105:50–4.
- [26] Ilanko S, Bharathy GK. Positive and negative penalty parameters in optimisation subjected to continuous constraints. *Comput Struct* 2012;108–109:83–92.
- [27] Ilanko S, Monterrubio L. *The Rayleigh–Ritz Method for Structural Analysis*. Hoboken, New Jersey: John Wiley & Sons, Inc; 2014.
- [28] Luenberger DG. *Optimization by Vector Space Methods*. New York: John Wiley & Sons; 1969.
- [29] Reddy J. *Applied Functional Analysis and Variational Methods in Engineering*. New York: McGraw Hill; 1986.
- [30] Zeidler E. *Nonlinear Functional Analysis and its Applications, vol III: Variational Methods and Optimization*. New York: Springer-Verlag; 1985.
- [31] Mikhlin S. *Variational Methods of Mathematical Physics*. New York: Mac Millan; 1964.
- [32] Rektorys K. *Variational Methods in Mathematics, Science and Engineering*. Dordrecht: Reidel Co; 1980.
- [33] Benabou MN, Margalef J, Outerlo E. *Análisis Matemático. Cálculo Integral en Espacios Euclídeos*. Ed. Pirámide, Madrid; 1982.